Swiss Journal of Geosciences (2019) 112:341–355
https://doi.org/10.1007/s00015-019-00339-0

# Unravelling the shape and stratigraphy of a glacially-overdeepened valley with reflection seismic: the Lienz Basin (Austria)

Thomas Burschil[1] · David C. Tanner[1] · Jürgen M. Reitner[2] · Hermann Buness[1] · Gerald Gabriel[1]

Received: 11 July 2018 / Accepted: 10 February 2019 / Published online: 12 March 2019


**Abstract**
We reveal the subsurface bedrock topography and sedimentary succession of one of the deepest glacially-formed basins in the Eastern Alps: the Lienz Basin in the Upper Drau Valley (Tyrol), by means of seismic reflection. A dense source-receiver spacing, supplied by autonomous receivers, and a prestack depth-migration processing scheme were essential to distinguish the various deposits in fine detail, such as slumping, fan delta deposits, and a modified monocline on the basin flank. These details support our interpretation of the seismic stratigraphy that consists of, e.g., subglacial till of last glacial maximum (LGM) age and possibly older, laminated basin fines, and gravel/coarse sand. The maximum depth of the basin is 622 m, at the junction of two major basement faults that are not clearly visible in the seismic reflections. We regard the overdeepening in this longitudinal valley as the result of glacier confluence during the LGM. Subglacial meltwaters utilized the higher erodibility of faulted rocks, as indicated by channel structures. The adverse slope (2.6%) along the valley axis exceeds the gradient ice-surface slope (0.4–0.5%) during the LGM by more than fivefold. We thus suggest this feature is a product of a pre-LGM phase, since adverse slopes greater than $\sim$ 1.2 times the ice surface slope promote the freezing of water in subglacial channels and prevent efficient water flushing of sediments. Integrating other studies allows us to estimate the local overdeepening of the Lienz Basin and that of the whole Upper Drau Valley to be 146 m and 530 m, respectively. At the beginning of lacustrine sedimentation, we estimate the paleo-water depth to be at least 216 m.

**Keywords** Seismic imaging · Seismic facies · Overdeepening · Basin morphology · Glacial sediments · Lienz Basin

## 1 Introduction

Overdeepened valleys and basins, with bedrock surfaces up to some hundred metres below the present landscape surface, are a common feature in areas that were affected by Quaternary glaciations (Huuse and Lykke-Andersen 2000; Preusser et al. 2010; Cook and Swift 2012). In principal, those overdeepenings are regarded as the legacy of several subglacial processes like abrasion (linked to basal sliding velocities), quarrying, and subglacial meltwater action (Hooke 1991; Alley et al. 2003; Benn and Evans 2010; Menzies et al. 2018). The first physical-based considerations of the formation of overdeepenings (Penck 1905) have been improved upon by numerical models. Such models range from simple ice-erosion simulation with a focus on ice-flow velocities (MacGregor et al. 2000; Anderson et al. 2006), to more sophisticated models that include hydrological-dependent ice-basal sliding and erosion (Herman et al. 2011) and different modes of subglacial sediment transport (Egholm et al. 2012). However, as the active subglacial environment does not allow the direct observation of glacial action, our understanding of the processes contributing to the formation of such subglacial basins is still speculative, despite more than a century of research. Key questions, such as why does overdeepening occur, what are the main processes involved, what controls their distribution (e.g. glaciological and lithological conditions), and at which specific stage of glaciation or landscape evolution are overdeepenings created, remain poorly answered (Cook and Swift 2012).

In the Alps, overdeepened features are mainly associated with tectonic structures, weak lithologies, and/or

Editorial handling: W. Winkler.

✉ Thomas Burschil
thomas.burschil@leibniz-liag.de

[1] Leibniz Institute for Applied Geophysics, Stilleweg 2, 30655 Hannover, Germany

[2] Geologische Bundesanstalt/Geological Survey of Austria, Neulinggasse 38, 1030 Vienna, Austria

Pleistocene ice confluences or diffluences (Preusser et al. 2010). In the Eastern Alps, two settings are characteristic: (1) Glacially-scoured basins in the ablation area of glaciers, e.g., the classical tongue basins (Penck and Brückner 1909). Prominent examples are the Salzach Basin that is filled with sediment (van Husen 1979; Pomper et al. 2017), or the lakes, Traunsee and Hallstätter See (van Husen 1979). (2) Buried elongated valleys in the so-called longitudinal valleys of the Eastern Alps (e.g. Inn, Salzach, Drau, and Enns Valleys). They follow the major strike-slip faults that formed in the course of the tectonic lateral extrusion towards the East during the Oligocene (Ratschbacher et al. 1991), and contain Oligocene sediments as well as Miocene syntectonic deposits (Frisch et al. 1998; 2000). GPS data (Grenerczy et al. 2005; Vrabec et al. 2006; Caporali et al. 2009) and active deformation in caves (Plan et al. 2010; Baroň et al. 2019) suggest that the tectonic eastward extrusion of the Eastern Alps, which waned during the late Middle Miocene (Frisch et al. 1998), is still active.

Overdeepened valleys are not only a feature of glacial erosion in an Alpine landscape, such as trimlines and (over-) steepened slopes. They have been sediment sinks on a local scale as well and are therefore archives of the environmental change, history of glaciation, denudation, and geohazards (e.g. catastrophic mass movements; Hinderer 2001; Dehnert et al. 2012; Starnberger et al. 2013; Grischott et al. 2017). The heterogeneous sedimentary fill of the Alpine valleys often constitutes a complex setting of deposits, with different facies, e.g. subglacial, (glacio-) lacustrine, deltaic (e.g., Hinderer 2001; van Husen and Mayer 2007; Fiebig et al. 2014; Buechi et al. 2018), and even rock slide deposits (Gruber et al. 2009). The histories of erosion and infill are even older than the last glacial cycle (Preusser et al. 2010; Reitner et al. 2010), which is not the only scientific interest. A rapidly expanding population and infrastructure in some inner-alpine valleys (e.g. Inn Valley, Lienz Basin) has awoken a vital societal interest for robust knowledge of subsurface conditions. This is a prerequisite, for instance, for groundwater protection from surface contamination, for ground motion prediction during seismic activity, and for engineering work, such as tunneling (Kovári and Fechtig 2004).

As boreholes are expensive, reflection seismic is the method of choice for a cost-effective exploration of such valleys. The sediment depths of these valleys (often $> 400$ m) usually require P-wave seismic methods, while the complexity of the sedimentary fill and the shape of the valley specify the reflection rather than refraction method, with as much resolution as is feasible. Seismic facies and velocities can be used to characterize sediments (Burschil et al. 2018), even if borehole information is not present.

In this paper, we present the first high-resolution reflection seismic profiles and interpretations of a strongly overdeepened longitudinal valley, i.e. the Lienz Basin, located in a high-mountainous landscape of southern Austria. Based on the seismic results and comparison with other studies in the surrounding overdeepened valleys, i.e. the Upper Drau Valley (Arndt and Bäk 2005; Brückl et al. 2010), the Hopfgarten Basin (Reitner et al. 2010), and the Salzach Valley (Pomper et al. 2017), we tackle the following key issues:

1. The link between the geometry of the overdeepening structure and the tectonic and paleo-glaciological conditions during its erosion.
2. The derivation of the depositional history of the basin based on its seismic stratigraphy.

## 2 Location and geological setting of the Lienz Basin

The Lienz Basin (LB) is geographically located in eastern Tyrol in southern Austria, at the confluence of the rivers, Isel and Drau (Fig. 1). It is surrounded on the western, northern, and eastern sides by the High Tauern mountain range (i.e. the Deferegger Alps, the Schober Group and the Kreuzeck Group, respectively), and on the southern side, it is bounded by the Southern Limestone Alps, i.e. the Lienz Dolomites.

Geologically, the area is part of the Austroalpine superunit (Schmid et al. 2004). All valley flanks of the LB consist of basement rocks (Schmid et al. 2004; Linner et al. 2013). The valleys of the Drau and Isel rivers follow the major strike-slip faults, which are the result of ductile and brittle deformation during the Oligocene to Miocene (Schmid et al. 1987; Schmidt et al. 1993; Favaro et al. 2015). The LB is located at the junction of two faults, i.e. the ESE-WNW striking Iseltal Fault, a synthetic fault of the Gailtal-Pustertal fault segment of the Periadriatic Fault system, and the ENE-WSW striking Drautal Fault related to the Zwischenbergen-Wölltratten Fault (Fig. 1a; Linner et al. 2009 and references within). The LB has a low seismicity (cf. Reiter et al. 2018); the faults of the LB are not known to be active. This is in contrast to the Periadriatic Fault, south of the Lienz Dolomites, which is still regarded active, as indicated by the Kartitsch Earthquake (24 km SW of Lienz, Fig. 1a) in 1862, with an I0 = 6.5° MSK, M = 4.4 (cf. Sprenger and Heinisch 1992).

During the Pleistocene glaciations, the Alps were covered by a complex of transection glaciers (van Husen 1987; Ehlers and Gibbard 2004; Reitner et al. 2016; Seguinot et al. 2018). During the last glacial maximum (LGM), the area of the LB was part of an accumulation area and the ice reached a maximum height of about 2200 m elevation,

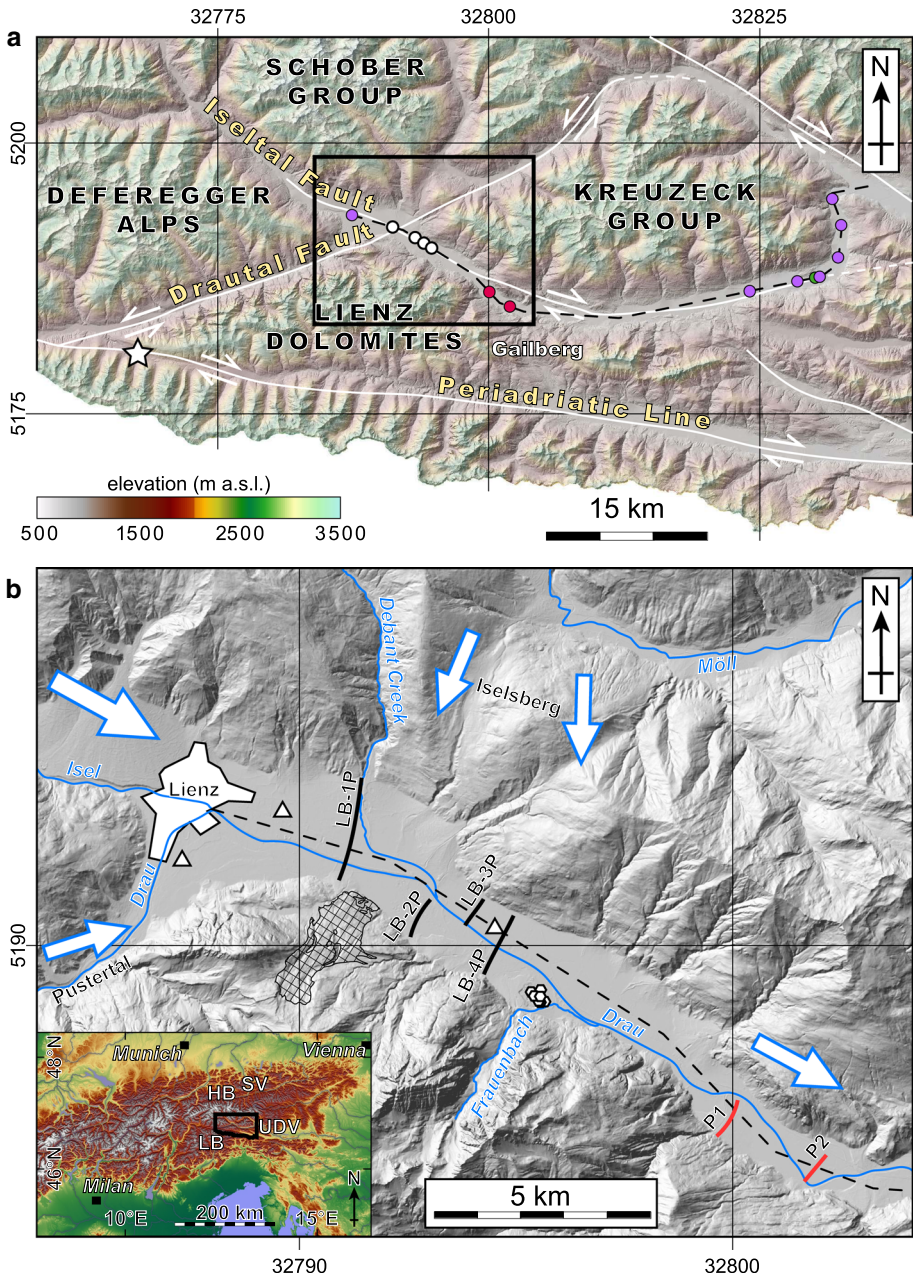


**Fig. 1** **a** Regional elevation map. White lines show major fault lineaments, a star marks the location of the Kartitsch Earthquake, and dashed line marks the line of longitudinal section along the Upper Drau Valley (Fig. 7b) with nodes for maximum valley depth from seismic sections presented here (white), seismic profiles of Brückl et al. (2010; red), gravimetric/refraction seismic data (Arndt & Bäk 2005; purple), and the Fellbach borehole (green). **b** Map of the Lienz Basin (LB). Blue arrows show major ice flow directions, black lines mark seismic profiles of this study and red lines those of Brückl et al. (2010). Triangles locate boreholes in the LB and hexagons at the Frauenbach alluvial fan. A cross-hatched polygon outlines the Holocene rock avalanche from the Lienz Dolomites. The insert map shows the location of the Upper Drau Valley (UDV), Hopfgarten Basin (HB), and Salzach Valley (SV). [DEM from https://www.data.gv.at/katalog/dataset/dgm; hill shape calculated from DEM]

based on trimline evidence (Reitner 2003a). The corresponding surface slope of the glacier along the valley axis was in the range of 0.4–0.5% (0.2°–0.3°), according to the reconstruction (van Husen 1987; Reitner 2003a).

The adjoining valley flanks are partly covered by subglacial till of last glacial maximum (LGM) age and deltaic deposits of ephemeral ice-dammed lakes of the subsequent early lateglacial phase of ice-decay (Reitner et al. 2016). In addition, the northern flank of the LB is characterized by deep-seated gravitational slope deformation because of glacial over-steepening. On the opposite side, however, a Holocene rock avalanche, with a volume of ca. 22 Mio $m^3$, descended from the Lienz Dolomites, just reaching the rim of the LB valley floor (Reitner 2003b; marked by cross-hatched polygon in Fig. 1b). The valley floor consists of fluvial gravel that is partly covered by silty overbank deposits. At the basin margins, streams of tributary valleys, such as the Debant Creek or the Frauenbach (Fig. 1b), have deposited alluvial fans.

The LB was the site of the confluence of the dominant Isel Glacier with branch glaciers of the Möll and Drau glaciers during the LGM. Penck and Brückner (1909) were the first to regard the LB as an overdeepened valley due to the obvious increase in valley width at the onset of the LB, NW of Lienz (Fig. 1), with respect to the upper parts of Isel and Drau Valley, and the presence of hanging valleys on

the flanks. Further indications of overdeepening of the LB were reported from a gravimetric survey conducted in the early 1990s (Walach 1993). Three boreholes in the LB (https://www.tirol.gv.at/statistik-budget/tiris/tiris-geodaten/; location marked by triangles in Fig. 1b) that reach down to 60 m below surface, show predominantly sandy gravel to cobble clasts, the clast lithologies are typical for the River Drau. This monotonous sediment succession is different from that found downstream near the Frauenbach alluvial fan. Multiple boreholes (hexagons in Fig. 1b), with a maximum depth of 55 m, prove the existence of a 10 m-thick package of fine sediments (backwater deposits), 40–50 m below surface, on top of fluvial deposits of the River Drau (Poscher and Patzelt 1995). According to $^{14}$C-data, the formation of the backwater deposits is the result of alluvial fan progradation during the Younger Dryas (YD; 12.8–11.7 ka). Taking all these data into account, the modern valley floor of the LB appears to have been in an aggradational phase since the YD, with the formation of terrace edges at the rim of alluvial fans only due to lateral erosion of the originally meandering River Drau.

## 3 Seismic reflection data

The Leibniz Institute for Applied Geophysics (LIAG) carried out a high-resolution, land-seismic reflection survey of the LB in 2016. We used a dense 2-D acquisition scheme of 5 m source and 2.5 m receiver spacing, in a split-spread/roll-along geometry. The hydraulic LIAG mini-vibrator HVP-30 (peak force ~ 30 kN) emitted two consecutive linear sweeps of 20–200 Hz for a 10 s duration per shot point. Vertical 20 Hz geophones (Sensor SM6) were planted and connected via cable to 15 Geometrics Geode seismographs. The Geodes performed field correlation with the excited sweep and recorded the seismograms from up to 360 channels with 1 ms sampling rate. In addition, we employed 60 planted geophones (Sensor SM6, 14 Hz, 3-component) connected to autonomous seismographs (Omnirecs DATA-CUBE$^3$) to fill gaps in the profiles, to extend the layout, and to record selected 3-D areas. The DATA-CUBE$^3$ recorded continuously with a 2.5 ms sampling rate.

The raw data shows visible reflections up to 700 ms, which indicate a very good data quality (Fig. 2). We identify a strong reflection of the basin floor and the steep flanks of the basin in all shots (red arrows in Fig. 2). Internal reflections are visible as well (blue arrows in Fig. 2). However, the northern part of LB-1P was measured on top of a 2-m high flood barrier that consists of large boulders. This causes a significant energy loss, visible in the raw data (marked green in Fig. 2).

Seismic processing was performed using SeisSpace software and the GIPPtools of GFZ German Research Centre for Geosciences, Potsdam. Raw data of the DATA-CUBE$^3$ were extracted according to the GPS-shot time and correlated with the excited sweep. Because each DATA-CUBE$^3$ started recording at a different initial time, we corrected all seismograms according to their particular static time-shift. Amplitudes were adjusted to the amplitudes of the data from Geode seismographs.

The raw data of the DATA-CUBE$^3$ and the Geodes were imported to SeisSpace and acquisition geometry for processing was assigned. We performed a processing sequence on a prestack depth migration level that produced the best results, according to visible structure and facies. The applied processing scheme comprises various steps, as shown by Bradford et al. (2006) and Burschil et al. (2018) for near-surface applications. It includes prestack processing with: (1) quality control, (2) muting of surface waves, (3) various static correction: (3.1) elevation statics to shift the seismograms to a processing datum, (3.2) the high frequency part of refraction statics (so that migration velocity analysis was able to adapt the shallow velocity field), and (3.3) residual statics, (4) spectral balancing to whiten the sweep frequencies (20–200 Hz), and (5) amplitude control that was carried out by correction of spherical divergence followed by automatic gain control of 300 ms window length.

We derived an initial velocity field from interactive velocity analysis of the prestack processed data. Since we expected an inhomogeneous velocity field and steeply-dipping valley flanks, we decided to apply prestack depth migration. We executed a Kirchhoff prestack depth migration from topography in common offset gathers on the prestack processed data. Several iterations of migration velocity analysis, combining horizon residual move-out analysis in the migrated common offset gather and a ray-based tomographic inversion (Stork 1992) were necessary to gain good results. Post-migration processing comprised spectral balancing, fk-filtering in the common-offset gathers and in the common-reflection-point gathers, severe top and bottom muting, and common-reflection-point stacking.

The use of additional DATA-CUBE$^3$ ensured a continuous 2-D profile and increased data quality significantly. Shallow layers were better imaged and vertical resolution was increased (marked purple in Fig. 3), since near offsets were available. Furthermore, the resolution in the deeper parts increased as well (marked blue in Fig. 3).

## 4 Seismic interpretation

All seismic sections show the interior of the LB in good detail (Fig. 4; highlights in Fig. 5). A reflector at the valley flanks marks the erosional base of the valley (blue line in Fig. 4), while it is challenging to determine the base of the basin in the deepest parts, since no distinct reflector occurs.

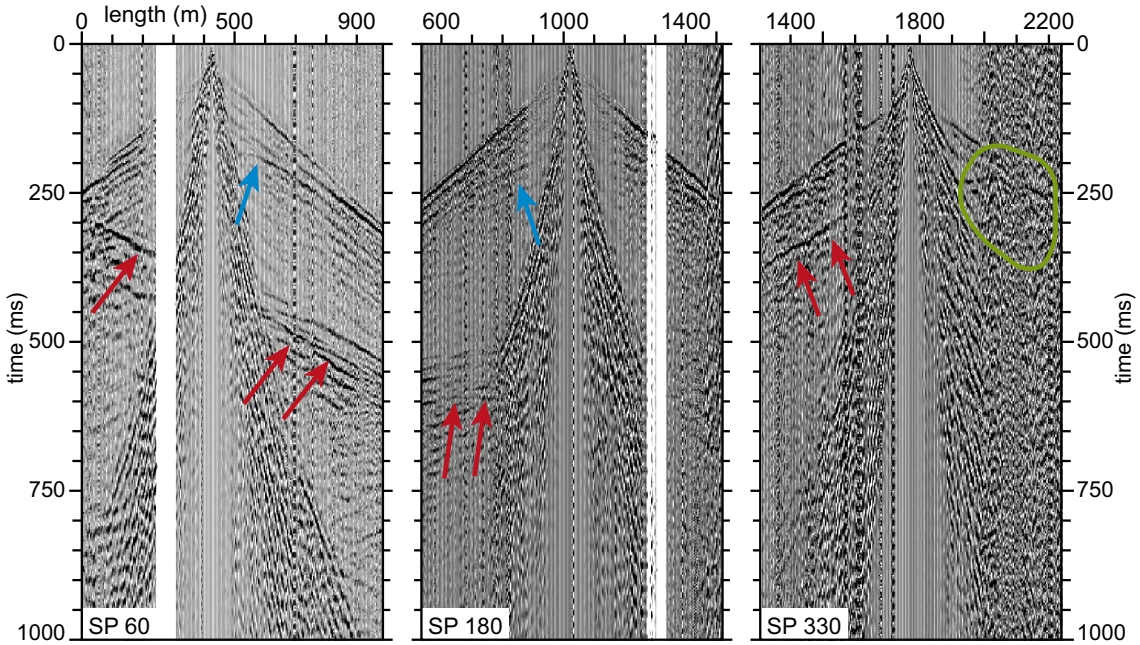


**Fig. 2** Examples of shot-gathers along profile LB-1P. White gaps are due to Drau River (@300 m) and maintenance depot (@1300 m). Red arrows mark reflection of valley flanks and base, blue arrows show reflections within the basin fill. Noise @1600 m is related to major road. Note the lower signal-to-noise ratio close to the flood barrier (green)

Here, we interpret the base of the LB as the transition downwards from the reflective part with high amplitude to the zone with medium to low amplitude, for which we give alternative interpretations (dashed blue lines in Fig. 4). The maximum valley depth varies from 622 m on LB-1P to 476 m on LB-3P (Table 1). From this we determine a local overdeepening of the LB of 146 m. Below the valley base, some seismic energy occurs. We can give two possible explanations for this energy: (1) it is energy from multiples or side reflections within the sediment succession of the basin or (2) it is reflected energy from below the basin. In the latter case, this diffuse, chaotic reflection pattern could be caused by the presence of the Iseltal Fault or a junction of this fault with other faults (Linner et al. 2009, 2013). Based on the areal overlap of the described features with the position of the faults, we regard the second explanation as the more probable.

### 4.1 Bedrock topography

Bedrock topographies in the valley cross-sections show a considerable variance within this short valley segment of only 3 km. Only cross section LB-4P (Fig. 4d) shows a symmetrical U-shape profile, which might be expected as the result of uniform subglacial erosion (Harbor 1992). In a downstream direction, the following development of valley profile is evident. The deepest bedrock elevation (ca. 30 m above the Adriatic (m AA), which corresponds to 622 m depth, cf. Table 1), south of the centre of the slightly asymmetric LB-1P-profile, can be followed as channel-like structures in LB-2P (ca. 140 m AA/512 m depth or ca. 70 m AA/585 m depth for the alternative interpretation) and LB-3P (ca. 175 m AA/476 m depth). Combing LB-2P and LB-3P it might even be possible to have two channel-like structures at different levels within one complete transect, which then disappear (or merge) in the LB-4P profile (Fig. 4). In total, there is a gentle but not constant 2.6% (1.5°) adverse subsurface slope from LB-1P to LB-4P. This development in geometry most probably reflects a combination of lithological and glaciological conditions. The biggest overdeepening in the LB occurs at the junction of the Iseltal Fault and the Drautal Fault, where faulted and thus relatively-weaker lithologies can be assumed. Consequently, these channel-like structures in LB-2P and LB-3P may have been incised into the Iseltal Fault towards SE.

### 4.2 Sedimentary succession

Within the sediment succession, the deepest layer (unit A, Fig. 4) has a maximum thickness of 85 m on LB-3P to 213 m on LB-2P, depending on the chosen interpretation. It shows high reflectivity, with reflector segments spanning 10 s of metres laterally. The seismic velocity of this layer (Fig. 6; Table 1) is significantly higher than the velocity of the layers above and indicates strong compaction, which is regarded as typical of subglacial sediments (Pfiffner et al. 1997; Büker et al. 1998; Reitner et al. 2010). Consequently, we interpret the deepest layer as a sediment package (unit

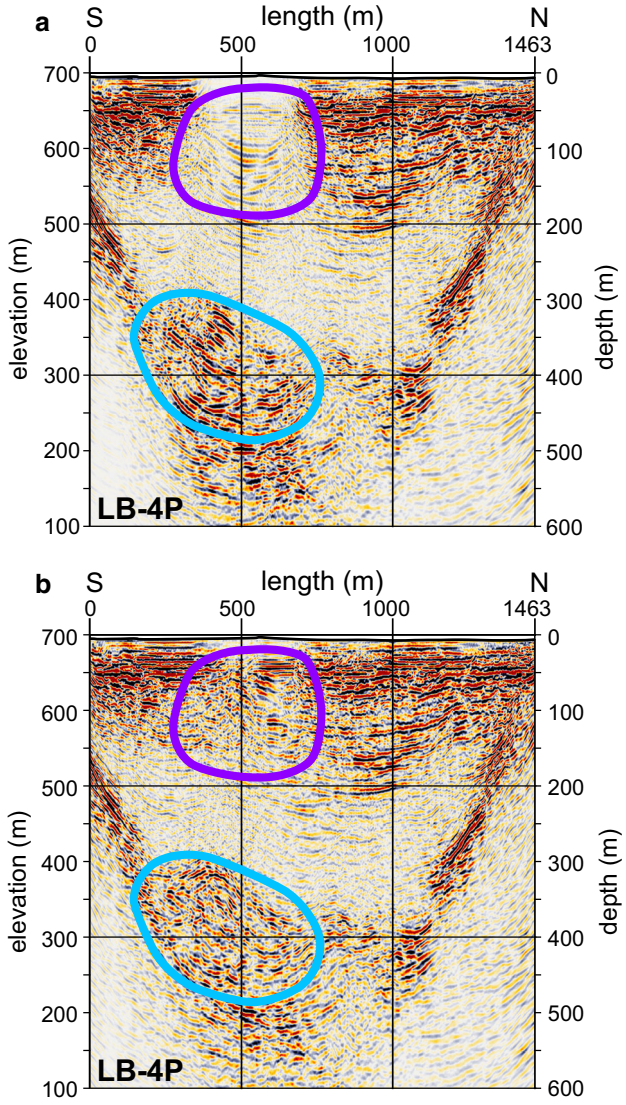


**Fig. 3** Comparison of PSDM without (**a**)/with (**b**) data from autonomous receivers. Imaging quality is improved in shallow (purple) and deep (cyan) regions

A), consisting of subglacial till and glaciolacustrine deposits such as waterlain till (massive dropstone mud to dropstone diamicton). We observe slumping structures within this deepest unit on the southern flanking profiles LB-1P (Fig. 5c) and LB-4P (Fig. 5e) that are characteristic features of (glacio-)lacustrine or comparable settings (Duncan 1996; Strasser et al. 2007), especially when considering the steep slopes (up to 35°) on the valley flanks.

Upwards, parallel reflectors with increasing amplitude occur unconformably on top of the subglacial till-package and onlap on the basin flanks (unit B, Fig. 4). This unit B shows higher thickness in the central part and lower thickness at the basin flanks. We interpret this unit as laminated basin fines in the sense of bottomset deposits, which have been found in the same seismofacies in other studies (Pfiffner et al. 1997; Reitner et al. 2010). It shows a depression at the centre of the basin that indicates compaction. More evidence for compaction is that the morphology of the reflectors follows the topography of the units above and the unit forms a monocline on the northern flank of LB-3P (Fig. 5d). The latter was modified by sedimentation from the flanks of the valley, which accentuated the monocline form. In addition, we interpret a coarse-grained delta deposit that wedges from the valley flank into the basin fines on the northern flank of LB-4P (Fig. 5f) and possibly at the northern flank of LB-3P (Fig. 5d). Deeply incised tributary valleys, NE of the seismic lines, indicate likely potential feeder systems for fan deltas in a deep-water lake. Surface analogues for such sedimentary architecture with delta deposits having steep foreset beds are present in the sedimentary record of the early Lateglacial Phase of ice-decay (Reitner et al. 2016).

Above unit B, we distinguish two layers (units C1 and C2) with different seismic facies (Fig. 4; close-up in Fig. 5a), separated by an unconformity (cyan line in Fig. 4). Their high reflectivity pattern contains reflector segments that are less than 100 m long, and they possess a higher frequency content than the reflector pattern of the laminated basin fines below. The lower layer (unit C1) contains clinoforms (Fig. 5b), indicating foreset beds, which are not present in the upper layer (unit C2). It shows a depression at the centre of the basin. The depression fill laterally onlaps/downlaps on to unit B, indicating an angular unconformity (Fig. 5a).

The layer above (unit D) lies unconformably on top of unit C2, in the central part of the valley (Fig. 5a). It shows a varying reflection pattern from profile to profile, with low frequency content and chaotic reflection on LB-1P and LB-3P (Fig. 4). This layer exhibits a higher seismic velocity on LB-1P and LB-3P than the surrounding units (Fig. 6; Table 1). In profile LB-1P, this unit thins towards the southern flank, where it finally disappears between the lower unit and the following upper unit. Moreover, the upper limit to the uppermost unit, in some of the profiles (LB-2P and LB-4P), is subhorizontal or has such segments (LB-1P and LB-3P).

Therefore we suggest three possible interpretations for unit D, which may be different for each profile: It either represents: (i) very coarse, clastic, fluvial deposits, (ii) a rock avalanche/rock slide deposit, or (iii) a till layer. All options consider the high velocities of this unit in LB-1P and LB-3P, which indicate strong compaction. The varying thickness and velocity of unit D from profile to profile shows the potential of sediments to change along the longitudinal axis of the LB. A very coarse, clastic, fluvial deposits (i) would be a topset above foreset beds (unit C), indicating the final phase of fill by deltaic sediments, which started with the bottomset beds of unit B. A possible

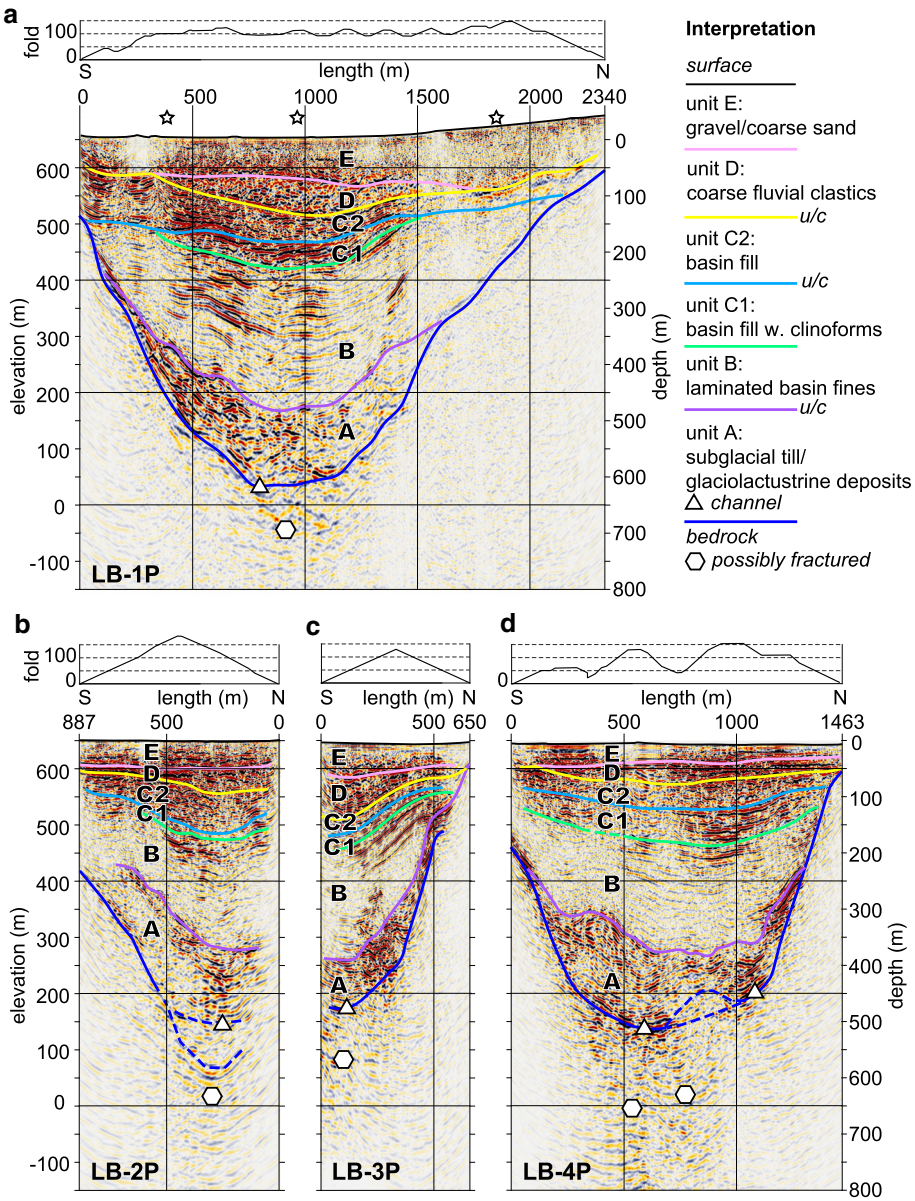


**Fig. 4** Interpreted seismic profiles LB-1P (**a**), LB-2P (**b**), LB-3P (**c**), LB-4P (**d**), and interpretation of sedimentary layers. 2.5 × vertical exaggeration. Dashed lines indicate alternative interpretations. Stars mark the shot locations in Fig. 2. White hexagons and triangles represent possible fractured rock and channels, respectively

transition to alluvial beds coming from the Debant Valley in profile LB-1P would be plausible. The second option, a rock avalanche/rock slide deposit (ii), could also show high velocities and chaotic structure (Brückl et al. 2010). However, a niche as the potential detachment area of such a catastrophic slope failure, which must have been considerably bigger than that of the known Holocene event (cf. Geological setting), is not apparent. A till layer (iii) as a result of a glacier re-advance would be unlikely, considering the chaotic internal structure. In addition, the geometry on the southern flank, with a conformable contact between the unit below and above, does not indicated any subglacial erosion event and corresponding unconformity linked to a glacier advance. Therefore, we regard fluvial formation for unit D, (option i), as the most plausible solution, although a contribution by gravitational processes cannot be ruled out completely.

The uppermost layer (unit E) shows a chaotic reflection pattern of high frequency content (Fig. 5a). This layer comprises gravels and coarse sand, as confirmed by the boreholes in the LB. Taking into account the results from boreholes in the Frauenbach alluvial fan, where the uppermost 50 m consists of deposits of YD age and younger on top of gravels of the river Drau, unit E is regarded as the uppermost fluvial layer.

Based on the seismic interpretation and the shape of the basin floor, we have derived a 3-D model of the Quaternary fill of the LB (Fig. 7a). The modelled layers follow the course of the basin and can be connected from profile to profile.

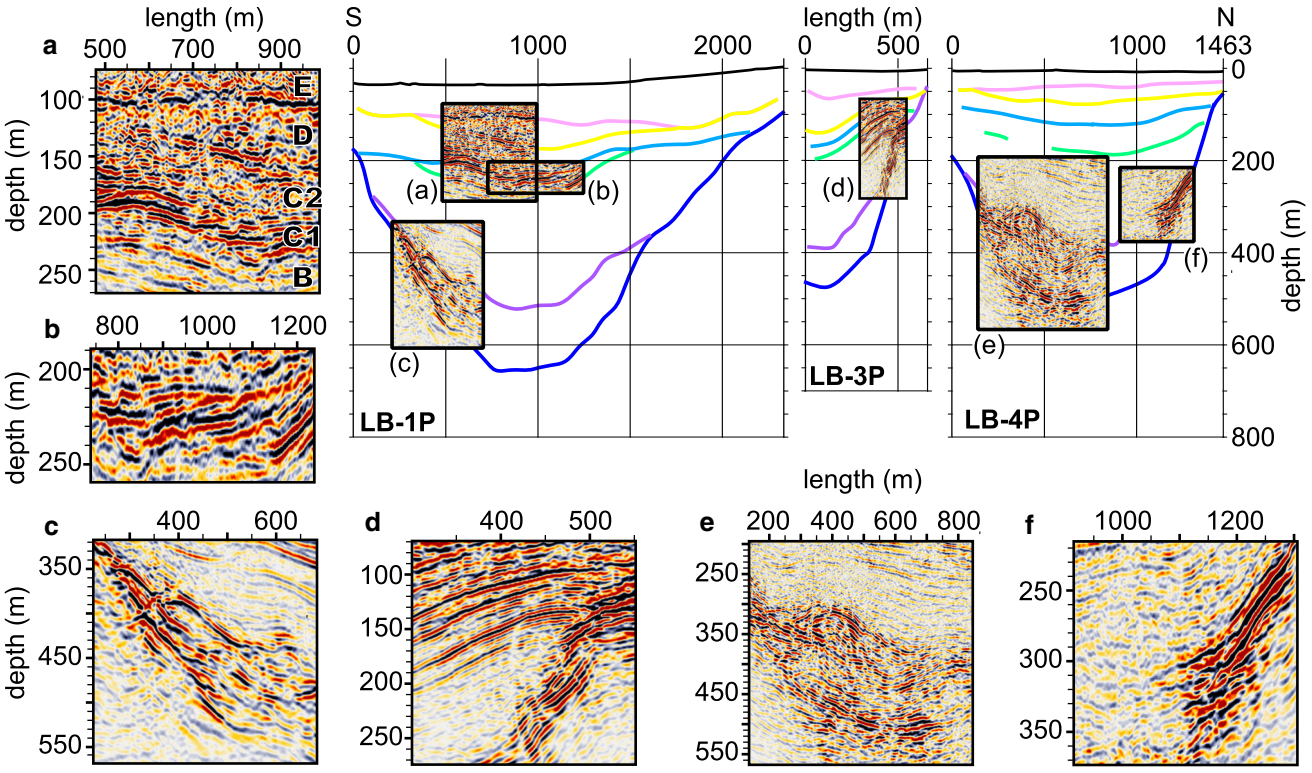


**Fig. 5** Highlighted reflection patterns: Sedimentary succession (**a**), onlap and foreset geometry in unit C1 (**b**), slumping structures in profile LB-1P (**c**) and LB-4P (**e**), modified monocline on basin flank (**d**), and alluvial fan (**f**)

## 5 Discussion of seismic results

Autonomous receivers, such as DATA-CUBE$^3$, are designed for passive seismic experiments, but see more and more application in active seismic experiments (e.g. Lay et al. 2016; Haberland et al. 2017). Combination of these seismographs with the cable-based Geometrics Geode recording system is rare. Brodic et al. (2015) showed the potential of combining autonomous and landstreamer-based receivers. The continuous profiling improved data quality significantly and was worth the effort (cf. Fig. 3). The data from both recording systems show similar data quality in terms of frequency and amplitude so that we do not notice a difference in recording quality.

The seismic interpretation was carried out using prominent reflectors and changes in seismic velocity and facies. A downward transition from high to medium/low reflectivity for the base of the basin is reported in other studies in the Alps (e.g. Nitsche et al. 2002; Dehnert et al. 2012; Fabbri et al. 2017). Since the interpretation of the valley base is not clear on all profiles, we suggest alternative interpretations of the valley base for LB-2P and in parts of LB-4P (Fig. 4b, d). Especially the reflectivity within the bedrock, below the valley base, complicates the interpretation. The direct detection of steep-dipping faults without marker horizons is challenging for the reflection seismic method. In addition, we optimized our field layout for seismic imaging of the sedimentary succession.

Seismic velocities of the infill of the LB range from 1679 m/s for shallow fluvial deposits to 2515 m/s for subglacial till and glaciolacustrine deposits (Table 1). Similar values for glacial, fluvial, and lacustrine deposits have been found by various studies with seismic reflection methods (Büker et al. 1998; Brückl et al. 2010; Pugin et al. 2014; Burschil et al. 2018) and full-waveform inversion (Bleibinhaus and Hilberg 2012). Velocities of unit D are higher on LB-1P and LB-3P, with respect to underlying units, which is in contrast to profiles LB-2P and LB-4P (cf. unit D in Seismic interpretation).

## 6 Comparison of the results with work carried out in surrounding overdeepened valleys

To put our findings into context, we first compare our results with recent comparable studies of surrounding valleys, beginning with the available data of the Upper Drau Valley (UDV) downstream of Lienz.

Investigations of the valley fill are rare in the UDV, from the LB down to the village of Sachsenburg. Only one deep borehole (Fellbach, OD II/3; https://gis.ktn.gv.at/

**Table 1** Maximum depths and average velocities of sedimentary units

| Unit | Facies | LB-1P | | | LB-2P | | | LB-3P | | | LB-4P | | |
|---|---|---|---|---|---|---|---|---|---|---|---|---|---|
| | | Depth (m) | Thickness (m) | Ø v (m/s) | Depth (m) | Thickness (m) | Ø v (m/s) | Depth (m) | Thickness (m) | Ø v (m/s) | Depth (m) | Thickness (m) | Ø v (m/s) |
| | | 0 | | | 0 | | | 0 | | | 0 | | |
| E | Gravel/coarse sand | 73 | 73 | 1736 | 49 | 49 | 1679 | 61 | 61 | 1839 | 30 | 30 | 1781 |
| D | Coarse fluvial clastics[#] | 134 | 61 | 2212 | 91 | 43 | 1786 | 140 | 79 | 2148 | 67 | 37 | 1825 |
| C2 | Basin fill | 183 | 49 | 1957 | 159 | 159 | 1828 | 171 | 30 | 2102 | 116 | 49 | 1862 |
| C1 | Basin fill w. clinoforms | 232 | 49 | 1876 | 171 | 12 | 1934 | 201 | 30 | 1963 | 177 | 61 | 1904 |
| B | Laminate basin fines | 488 | 256 | 1930 | 372 | 201 | 2016 | 390 | 189 | 1802 | 372 | 195 | 1874 |
| A | Subglacial till/glaciolacustine deposits | 622 | 134 | 2515 | 512/585* | 140/213* | 2478 | 476 | 85 | 2322 | 512 | 140 | 2214 |

Maximum bedrock depth of alternative interpretations are given for LB-2P

*Maximum depth depends on interpretation

#Alternative options for interpretation

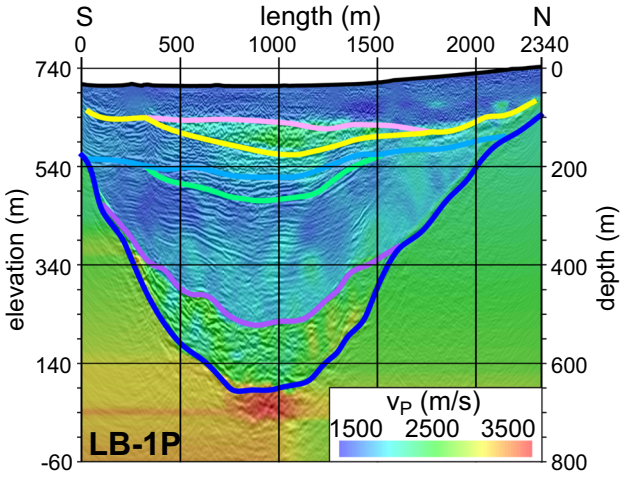


**Fig. 6** Seismic velocity from migration velocity analysis of LB-1P

atlas/) exists 42 km downstream of Lienz, which did not reach bedrock at 200 m depth (Ucik 2005). A review of complementary geophysical surveys in the adjoined part of the UDV (Arndt and Bäk 2005, and references therein) reported bedrock at depths of 400–700 m below surface. In this review, the maximum depth is suggested to be about 15 km downstream of Lienz (cf. Fig. 1; Brückl et al. 2010) at 700 m depth (− 100 m AA), while the highest bedrock elevation is located west of Sachsenburg, at 140 m depth (430 m AA). Thus, the regional overdeepening of the UDV reaches 530 m (Fig. 7b). The highest bedrock elevation, west of Sachsenburg, also marks the minimum elevation for the paleo-lacustrine level. We can therefore estimate a minimum water depth of 216 m at the beginning of the deposition of the basin fines (unit B), which shows its deepest level of 214 m AA at LB-1P. Nevertheless, the laminated basin fines (unit B) reach thicknesses of up to 256 m.

The closest seismic investigation to our study is that of Brückl et al. (2010; Fig. 1). They interpreted seismic reflection and gravimetric results and estimate a sedimentary succession of three units: The deepest unit, addressed as “old valley-fill”, is separated from lacustrine sediments above by a significant, curved-shaped boundary at ∼ 330 m depth. Brückl et al. (2010) assume that this boundary represents the glacier bed of the LGM. At this boundary, the reflection pattern changes from distinct, sub-horizontal reflectors in deeper to high frequency continuous reflections in upper parts. The uppermost layer of 40 m thickness corresponds to gravel and sand.

In the LB, we are able to image the sediment succession in more detail than Brückl et al. (2010), in particular a more detailed morphology of the layers. We identify the deepest layer (unit A) as deposits consisting of subglacial till and glaciolacustrine sediments, which may correspond

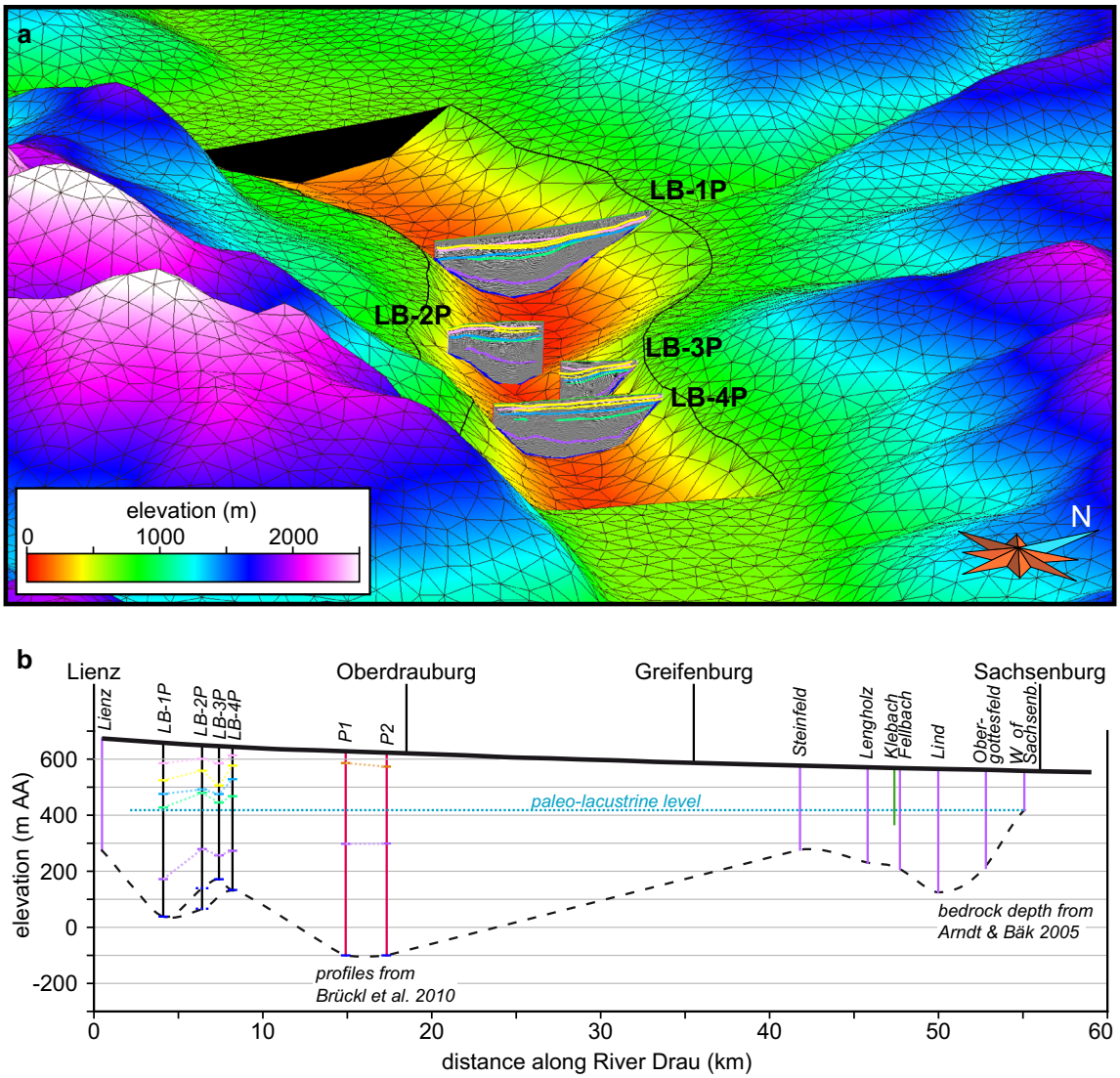


**Fig. 7** 3-D model of bedrock geometry and interpreted seismic profiles with elevation colour-coded (**a**). Longitudinal cross-section along the Upper Drau Valley (**b**) (for location of nodes, see Fig. 1a). Vertical lines show maximum depth of bedrock from seismic data of this study (black), and of Brückl et al. (2010) (red), from geophysical data (purple), summarized in Arndt and Bäk (2005). The Fellbach borehole (green) did not reach the bedrock. Colours shown in profiles LB-1P–LB-4P are given in Fig. 4

to the "old valley-fill" of Brückl et al. (2010), overlain by lacustrine deposits (our unit B). Internal structures within this layer are visible in our data, but difficult to interpret in the UDV. At both locations, this layer shows increased seismic velocity. The unit thickens from ca. 140 m in the LB to 380 m in the profiles of Brückl et al. (2010; cf. Fig. 7). Hence, our results allow a correlation of subsurface strata downstream and suggest the deposition of the valley infill within one glacial cycle, in contradiction to the conclusions of Brückl et al. (2010). A comparison of bedrock geometry along the valley show a similar shape for the LB (LB-4P; Fig. 4d) and the UDV (Fig. 3 in Brückl et al. 2010).

The overdeepened Hopfgarten Basin (HB; cf. overview map in Fig. 1), located to the North of the High Tauern mountain range, shows a more diverse sediment succession, which was interpreted as the result of at least three glacial cycles, based on a combination of geoelectrical and seismic data correlated with geological evidence from the surface (Reitner et al. 2010). Unsorted coarse-grained deposits occur in the deepest parts of the HB, showing a nearly transparent seismic facies, whereas the deepest sediments in the LB are highly reflective. The thick layer of laminated basin fines in the LB is not present in the HB. Unconformities terminate layers with clinoforms in both basins. Unit D of the LB is thicker than in the HB, where all basal till layers are often less than a single reflection (estimated $> 5$ m; Reitner et al. 2010). The uppermost deposits in the HB are deltaic fore- and topsets that

laterally grade into alluvial fan or fan delta deposits, whereas the upper beds in the LB are gravels and coarse sand.

Pomper et al. (2017) determined the bedrock geometry of the Lower Salzach Valley (SV; cf. overview map in Fig. 1), located in a classical tongue basin position, from drill logs, seismic, and valley-side slope data. Their detailed bedrock model shows two troughs along the SV, whereas there are at least three troughs in the UDV (Fig. 7b). The SV fill consists of fluvial, lacustrine, and basal moraine deposits. Coarse-grained delta deposits dominate the infill of the proximal southern part of the valley, while coarse-grained sediments are less prominent in the more distal northern part. Therefore, Pomper et al. (2017) assume rapid sedimentation of the overdeepened valley, before coarse-grained fluvial sediments were able to be delivered to the northern part of the valley.

A distinct reflection of the bedrock is reported for other valleys (e.g., Reitner et al. 2010), while we determine the valley base to be at the transition of the seismic reflective to transparent region. All valleys discussed here show subglacial sediments followed by lacustrine and fluvial deposits, even if the HB preserves sediments of different glaciations. In summary, the bedrock topography of the LB fits well to that of the UDV. A set of troughs can be detected in the proximal UDV, similar to the more distal SV.

The seismic facies of the LB has a similar character to that of the seismic facies of the Tannwald Basin, which is a distal branch basin of the Rhine Glacier that we investigated using the same acquisition parameters (Burschil et al. 2018). Other studies have shown similar seismic facies for the glacial, fluvial, and lacustrine deposits in overdeepened valleys (e.g., Büker et al. 1998; Brückl et al. 2010). The shape and depression of the layers of the basin fines interpreted in the LB can also be identified in other overdeepened, lacustrine environments (e.g., van Rensbergen et al. 1998).

## 7 Formation and depositional sequence of the LB—a synthesis

The biggest overdeepening of the LB occurs in the southern part of LB-1P, at the junction of the Iseltal Fault and the Drautal Fault, where faulted and thus relatively weaker lithologies can be assumed. Combining the geometries in a downstream direction, and thus in the former ice flow direction, the following development can be recognized: (1) there is a gentle, but not constant 2.6% adverse subsurface slope from LB-1P to LB-3P. (2) The profiles develop from asymmetrical (LB-1P) to resembling channels (LB-2P and LB-3P) to, finally, a U-shaped profile (LB-4P). The latter might be regarded as a result of the merged channels in LB-2P and LB-3P. This development in geometry most probably reflects a combination of lithological and glaciological conditions. Consequently, the incised channel-like structure in LB-2P displays the trace of the Iseltal Fault towards SE (triangle in Fig. 4). In addition, the peculiar geometries of LB-2P and LB-3P can be best explained by erosion through subglacial meltwater streams, which utilized the higher erodibility of the faulted rocks. Such linear features are common in the subglacial environments, as documented in other overdeepened structures as well (Benn and Evans 2010, and references within). It is remarkable, that the adverse slopes (2.6%) exceeds the gradient of the ice-surface slope at the LB (0.4–0.5%) during the LGM by more than fivefold. However, adverse slopes greater than $\sim$ 1.2 times the ice surface slope promote the freezing of water in subglacial channels and, hence, will prevent efficient water flushing of sediment (Röthlisberger 1972; Röthlisberger and Lang 1987; Hooke 1991; Creyts and Clarke 2010; see also discussion in Cook and Swift 2012). This discrepancy may be an indication for the formation of such subglacial meltwater features and, thus, of at least parts of the overdeepening during glacial phases with a different glacier geometry in the LB compared to LGM conditions. This was most likely the case quite early during the LGM or a previous glaciation, as advancing glaciers have in general steeper ice surface slopes, at least at the tongue, than those during the climax of a glaciation. During a phase of smaller glacier size, in the course of the last glacial cycle or before, the LB might have been covered by a glacier tongue, which was then part of the ablation zone and not, like during the LGM climax, part of the accumulation area. Such a situation increases the abundance of subglacial water and, thus, the erosion capacity of the paleo-glacier (Cook and Swift 2012).

From the overall paleo-glaciological and paleo-geographical point of view, the LB reflects a glacier confluence; that of the dominant glacier coming from the Isel Valley with the branch of the Möll Valley overflowing the low transfluence pass of Iselsberg to the South. The contribution from the Pustertal, west of Lienz, is regarded as subordinate, in accordance with the suggestion of Penck and Brückner (1909). The effect of the confluence at LB is also visible in the ice flow model (Seguinot et al. 2018; cf. video of ice flow), where the highest ice flow velocities, the major factor contributing to glacial erosion, is evident in the LB and its prolongation to UDV. The velocity decreases down-flow of the UDV, only when the first diffluence occurs via a transfluence pass (Gailberg Saddle; Fig. 1a).

The infill, consisting six units (A-E), provides some information about the contributing processes. The more

than 100 m thick unit A shows a complex of subglacial and glaciolacustrine deposits (waterlain till/dropstone mud to dropstone diamicton), with slumping structures coming from the valley flanks. It is a matter of speculation whether there were a number of subglacial till layers deposited during one glaciation, which can be the result of decoupling of the glacier with meltwater-influenced deposition followed by re-coupling, as suggested by Buechi et al. (2017) to explain a decametres and thicker diamicton association in a Swiss glacially-shaped bedrock trough. Such a style of subglacial emplacement, which easily explains the high velocities of a thick package, is regarded as the effect of fluctuating water pressures at the ice–bed interface. A reverse-gradient of the subsurface bedrock topography, as well as the narrowing of the valley in the ice-flow direction may have promoted high basal pressures in an overdeepened bedrock trough, such as the LB. However, without a borehole we cannot rule out that there may be a remnant of a till formed during an older glaciation at the base of unit A.

With unit B, a bottomset deposit, the formation of a lake, and hence, the disappearance of the previous ice cover can be reconstructed. The sharp contact between the units A and B could be the result of rapid thinning of a stagnant ice body during deglaciation, leading to a sudden loss of bed contact of the remaining dead ice body due to ice floatation. Similar models have been proposed for Alpine valleys to explain rapid ice-decay based on sedimentary and morphological features on the valley flanks (e.g., van Husen 2000; Reitner 2007). According to this model, the bottomset bed most likely resembles the transition from glaciolacustrine conditions with floating icebergs of the collapse dead ice and deposition of dropstones to, eventually, lacustrine conditions. The thickness of more than 200 m is not an indication of a lake phase lasting some 1000 years. The dominance of crystalline rocks, especially schists, in the catchment of the River Drau, which delivers abundant fine material into the suspension load, provides an easy explanation for such thick bottomsets.

Fan delta deposits at the flanks of unit B show the input of coarser material, which then proceeded with the dominance of delta foresets (in unit C). The nature of unit D is, in some parts, elusive due to the presence of higher velocities and chaotic structures, which might be seen as an indication of a deposit of a glacial re-advance. Instead, we prefer an interpretation of a fluvial deposit, in the sense of a topset bed, made up of coarse gravel and cobble as the backfill of the lake in the LB. Renewed fluvial-style aggradation resulted in the formation of unit E with a thickness of 50–60 m. Data from Frauenbach alluvial-fan boreholes indicate the onset of this process in the YD (Poscher and Patzelt 1995).

According to this sedimentary succession and the proposed relative chronology of processes, the last glacial shaping of the LB took place in the LGM, followed by rapid infill during the Alpine Lateglacial (19–11.7 ka). The following lake phase, caused by rapid deglaciation during the phase of ice-decay, ended at least before the YD, according to the oldest available radiocarbon ages. Considering data from other overdeepened valleys (van Husen 1979), an infill over some few 1000 years after deglaciation seems to be possible. Ongoing aggradation, predominantly climatically steered (Patzelt 1987), since at least the YD, resulted in the formation of the youngest unit of the LB.

This model of a last glacial erosion of the LB in a prominent confluence during the LGM is supported by ice-flow modelling for the LGM (Seguinot et al. 2018). However, we cannot rule out the possibility of remnants of older glaciations in the sense of till and glacio-lacustrine deposits within the lowest unit.

## 8 Conclusions

We were able to acquire high quality seismic reflection data from the Lienz Basin. The prestack depth migration processing strategy proved capable to image the sedimentary succession of the 600 m thickness. The dense acquisition scheme, in combination with a small seismic vibrator source, enables high-resolution imaging of the bedrock and the Quaternary basin fill. The seismic survey benefited from additional autonomous receivers that filled gaps in areas where we could not deploy standard acquisition equipment.

On the basis of the data, we link the formation of the LB to the regional geology of faulted and, thus, weakened bedrock. Our data contribute to visualize the remarkable overdeepening in the UDV, as the result of the enhanced glacial erosion at the confluence of three Pleistocene glaciers, preconditioned by the tectonic setting with the greatest overdeepening located at the junction of two strike-slip basement faults. The higher erodibility of faulted and, thus, weakened rock is also evident in small-scale erosional features. The location of channels due to erosion by subglacial meltwater, would seem to follow the trace of faults.

The adverse slopes (2.6%) of the basin exceeds the gradient of the ice-surface slope at the LB (0.4–0.5%) during the LGM more than fivefold, which is far beyond the threshold of 1.2 times, above which the freezing of water in subglacial channels occurs with a negative effect on sediment flushing. This discrepancy is an indication that the glacial overdeepening, of at least some parts of the LB, might have taken place before the climax of the glaciation

or during a previous glaciation with a different glacier geometry and a corresponding steeper ice surface slopes.

The seismic stratigraphy reveals the sedimentary succession of the LB, even if it has not yet been calibrated by borehole information. The fine detail in the seismic images is necessary to depict features such as slumping within the subglacial till/glaciolacustrine deposits layer, a fan delta wedging into the laminated basin fines, and clinoforms in the basin fill. This allows us to derive the depositional sequence for six units in the LB. We are able to correlate the lowest unit (waterlain sub-glacial till) with that of Brückl et al. (2010), 15 km downstream in the UDV. We determine a local overdeepening of 146 m within the LB and a regional overdeepening of 530 m for the UDV. Furthermore, we are able to postulate a water depth of at least 216 m at the beginning of deposition of unit B.

In summary, the structure of the LB can be explained by subglacial erosion preconditioned by the tectonic setting. Based on the conspicuous subsurface bedrock surface and the great thickness of the lowermost subglacial till/glaciolacustrine deposit layer, the geometry and infill might document glacial phases prior to the LGM. However, a deep borehole is needed to overcome these speculations.

**Acknowledgements** The project was funded by German Research Foundation DFG, Grants KR2073/3-1, GA749/5-1, BU2467/1-2. We acknowledge the Geophysical Instrument Pool Potsdam at the GFZ German Research Centre for Geosciences Helmholtz Centre Potsdam for providing seismic equipment, Grant GIPP201623, and the help of Christian Haberland and Manfred Stiller. We thank our colleagues, among others, Markus Fiebig (BOKU Vienna), Harald Haider and Andreas Gander (Baubezirksamt Lienz), and Paul Herbst (GWU) for support and advice; Philip Nagy and the LIAG field crew, who carried out the seismic surveys and Manfred Linner for discussions on the tectonic setting. A special thanks to the editor-in-chief Wilfried Winkler and the reviewers, Darell A. Swift and Wilfried Gruber, who carefully revised and improved our manuscript.



## References

Alley, R. B., Lawson, D. E., Larson, G. J., Evenson, E. B., & Baker, G. S. (2003). Stabilizing feedbacks in glacier-bed erosion. *Nature, 424,* 758–760.

Anderson, R. S., Molnar, P., & Kessler, M. A. (2006). Features of glacial valley profiles simply explained. *Journal of Geophysical Research: Earth Surface, 111,* F01004.

Arndt, R., & Bäk, R. (2005). Geophysik im Drautal-Ergebnisse und Erkenntnisse. In R. Schuster (Ed.), *Arbeitstagung 2005 der Geologischen Bundesanstalt Blatt 182 Spittal an der Drau, Gmünd/Kärnten 12.-16. Sept. 2005* (pp. 103–115), Vienna: Geologische Bundesanstalt.

Baroň, I., Plan, L., Sokol, L., Grasemann, B., Melichar, R., Mitrovic, I., et al. (2019). Present-day kinematic behaviour of active faults in the Eastern Alps. *Tectonophysics, 752,* 1–23.

Benn, D. I., & Evans, D. J. A. (2010). *Glaciers and glaciation* (p. 802). London: Hodder Education.

Bleibinhaus, F., & Hilberg, S. (2012). Shape and structure of the Salzach Valley, Austria, from seismic traveltime tomography and full waveform inversion. *Geophysical Journal International, 189,* 1701–1716.

Bradford, J., Liberty, L., Lyle, M., Clement, W., & Hess, S. (2006). Imaging complex structure in shallow seismic-reflection data using prestack depth migration. *Geophysics, 71*(6), B175–B181.

Brodic, B., Malehmir, A., Juhlin, C., Dynesius, L., Bastani, M., & Palm, H. (2015). Multicomponent broadband digital-based seismic landstreamer for near-surface applications. *Journal of Applied Geophysics, 123,* 227–241.

Brückl, E., Brückl, J., Chwatal, W., & Ullrich, C. (2010). Deep alpine valleys: examples of geophysical explorations in Austria. *Swiss Journal of Geosciences, 103,* 329–344.

Buechi, M. W., Frank, S. M., Graf, H. R., Menzies, J., & Anselmetti, F. S. (2017). Subglacial emplacement of tills and meltwater deposits at the base of overdeepened bedrock troughs. *Sedimentology, 64*(3), 658–685.

Buechi, M. W., Graf, H. R., Haldimann, P., Lowick, S. E., & Anselmetti, F. S. (2018). Multiple Quaternary erosion and infill cycles in overdeepened basins of the northern Alpine foreland. *Swiss Journal of Geosciences, 111*(1–2), 133–167.

Büker, F., Green, A. G., & Horstmeyer, H. (1998). Shallow seismic reflection study of a glaciated valley. *Geophysics, 63,* 1395–1407.

Burschil, T., Buness, H., Tanner, D. C., Wielandt-Schuster, U., Ellwanger, D., & Gabriel, G. (2018). High-resolution reflection seismics reveal the structure and the evolution of the Quaternary glacial Tannwald Basin. *Near Surface Geophysics, 16,* 593–610.

Caporali, A., Aichhorn, C., Barlik, M., Becker, M., Fejes, I., Gerhatova, L., et al. (2009). Surface kinematics in the Alpine–Carpathian–Dinaric and Balkan region inferred from a new multi-network GPS combination solution. *Tectonophysics, 474*(1–2), 295–321.

Cook, S. J., & Swift, D. A. (2012). Subglacial basins: Their origin and importance in glacial systems and landscapes. *Earth Science Reviews, 115*(4), 332–372.

Creyts, T. T., & Clarke, G. K. (2010). Hydraulics of subglacial supercooling: Theory and simulations for clear water flows. *Journal of Geophysical Research: Earth Surface, 115,* F03021.

Dehnert, A., Lowick, S. E., Preusser, F., Anselmetti, F. S., Drescher-Schneider, R., Graf, H. R., et al. (2012). Evolution of an overdeepened trough in the northern Alpine Foreland at Niederweningen, Switzerland. *Quaternary Science Reviews, 34,* 127–145.

Duncan, J. M. (1996). State of the art: Limit equilibrium and finite-element analysis of slopes. *Journal of Geotechnical and Geoenvironmental Engineering, 122*(7), 577–596.

Egholm, D. L., Pedersen, V. K., Knudsen, M. F., & Larsen, N. K. (2012). Coupling the flow of ice, water, and sediment in a glacial landscape evolution model. *Geomorphology, 141,* 47–66.

Ehlers, J., & Gibbard, P. L. (2004). *Quaternary glaciations—extent and chronology: Part I: Europe* (p. 488). Amsterdam: Elsevier.

Fabbri, S. C., Herwegh, M., Horstmeyer, H., Hilbe, M., Hübscher, C., Merz, K., et al. (2017). Combining amphibious geomorphology with subsurface geophysical and geological data: A neotectonic study at the front of the Alps (Bernese Alps, Switzerland). *Quaternary International, 451,* 101–113.

Favaro, S., Schuster, R., Handy, M. R., Scharf, A., & Pestal, G. (2015). Transition from orogen-perpendicular to orogen-parallel exhumation and cooling during crustal indentation—Key constraints from $^{147}Sm/^{144}Nd$ and $^{87}Rb/^{87}Sr$ geochronology (Tauern Window, Alps). *Tectonophysics, 665,* 1–16.

Fiebig, M., Herbst, P., Drescher-Schneider, R., Lüthgens, C., Lomax, J., & Doppler, G. (2014). Some remarks about a new Last Glacial record from the western Salzach foreland glacier basin (Southern Germany). *Quaternary International, 328,* 107–119.

Frisch, W., Dunkl, I., & Kuhlemann, J. (2000). Post-collisional orogen-parallel large-scale extension in the Eastern Alps. *Tectonophysics, 327*(3–4), 239–265.

Frisch, W., Kuhlemann, J., Dunkl, I., & Brügel, A. (1998). Palinspastic reconstruction and topographic evolution of the Eastern Alps during late Tertiary tectonic extrusion. *Tectonophysics, 297*(1–4), 1–15.

Grenerczy, G., Sella, G., Stein, S., & Kenyeres, A. (2005). Tectonic implications of the GPS velocity field in the northern Adriatic region. *Geophysical Research Letters, 32*(16), L16311.

Grischott, R., Kober, F., Lupker, M., Reitner, J. M., Drescher-Schneider, R., Hajdas, I., et al. (2017). Millennial scale variability of denudation rates for the last 15 kyr inferred from the detrital $^{10}Be$ record of Lake Stappitz in the Hohe Tauern massif. *Austrian Alps. The Holocene, 27*(12), 1914–1927.

Gruber, A., Strauhal, T., Prager, C., Reitner, J. M., Brandner, R., & Zangerl, C. (2009). Die "Butterbichl-Gleitmasse"—eine große fossile Massenbewegung am Südrand der Nördlichen Kalkalpen (Tirol, Österreich). *Swiss Bulletin für angewandte Geologie, 14,* 103–134.

Haberland, C., Gibert, L., Jurado, M. J., Stiller, M., Baumann-Wilke, M., Scott, G., et al. (2017). Architecture and tectono-stratigraphic evolution of the intramontane Baza Basin (Bétics, SE-Spain): Constraints from seismic imaging. *Tectonophysics, 709,* 69–84.

Harbor, J. M. (1992). Numerical modeling of the development of U-shaped valleys by glacial erosion. *Geological Society of America Bulletin, 104*(10), 1364–1375.

Herman, F., Beaud, F., Champagnac, J. D., Lemieux, J. M., & Sternai, P. (2011). Glacial hydrology and erosion patterns: A mechanism for carving glacial valleys. *Earth and Planetary Science Letters, 310*(3–4), 498–508.

Hinderer, M. (2001). Late Quaternary denudation of the Alps, valley and lake fillings and modern river loads. *Geodinamica Acta, 14*(3–4), 231–263.

Hooke, R. L. (1991). Positive feedbacks associated with erosion of glacial cirques and overdeepenings. *Geological Society of America Bulletin, 103*(8), 1104–1108.

Huuse, M., & Lykke-Andersen, H. (2000). Overdeepened Quaternary valleys in the eastern Danish North Sea: Morphology and origin. *Quaternary Science Reviews, 19,* 1233–1253.

Kovári, K., & Fechtig, R. (2004). *Historische Alpendurchstiche in der Schweiz (140 pp)*. Zürich: Zürich & Gesellschaft für Ingenieurbaukunst, Stäubli AG Verlag.

Lay, V., Buske, S., Lukács, A., Gorman, A. R., Bannister, S., & Schmitt, D. R. (2016). Advanced seismic imaging techniques characterize the Alpine Fault at Whataroa (New Zealand). *Journal of Geophysical Research (Solid Earth), 121*(12), 8792–8812.

Linner, M., Habler, G., & Grasemann, B. (2009): Switch of kinematics in the Austroalpine basement between the Defereggen–Antholz–Vals (DAV) and the Pustertal–Gailtal fault-Eastern Alps. Alpine Workshop 2009, Cogne/Italy 16–19 September 2009. https://www.geologie.ac.at/fileadmin/user_upload/dokumente/pdf/poster/poster_2009_alp_shop_09.pdf. Accessed date July 06, 2018.

Linner, M., Reitner, J. M., & Pavlik, W. (2013). Geologische Karte der Republik Österreich 1:50.000 Blatt 179 Lienz. Wien: Geologische Bundesanstalt.

MacGregor, K. R., Anderson, R. S., Anderson, S. P., & Waddington, E. D. (2000). Numerical simulations of glacial-valley longitudinal profile evolution. *Geology, 28*(11), 1031–1034.

Menzies, J., van der Meer, J. J. M., & Shilts, W. W. (2018). Subglacial processes and landforms. In J. Menzies, & J.J.M. van der Meer (Eds.) *Past Glacial Environments* (pp. 105–158). Elsevier, Amsterdam.

Nitsche, F. O., Green, A. G., Horstmeyer, H., & Büker, F. (2002). Late Quaternary depositional history of the Reuss delta, Switzerland: Constraints from high-resolution seismic reflection and georadar surveys. *Journal of Quaternary Science: Published for the Quaternary Research Association, 17*(2), 131–143.

Patzelt, G. (1987). Untersuchungen zur nacheiszeitlichen Schwemmkegel-und Talentwicklung in Tirol. *Veröffentlichungen des Museums Ferdinandeum, 67,* 93–123.

Penck, A. (1905). Glacial features in the surface of the Alps. *The Journal of Geology, 13*(1), 1–19.

Penck, A., & Brückner, E. (1909). *Die Alpen im Eiszeitalter* (p. 1199). Leipzig: Tauchnitz.

Pfiffner, O. A., Heitzmann, P., Lehner, P., Frei, W., Pugin, A., & Felber, M. (1997). Incision and backfilling of Alpine valleys: Pliocene, Pleistocene and Holocene processes. In O. A. Pfiffner, P. Lehner, P. Heitzmann, S. Mueller, & A. Steck (Eds.), *Deep structure of the Swiss Alps: Results of NRP 20* (pp. 265–288). Basel: Birkhäuser.

Plan, L., Grasemann, B., Spötl, C., Decker, K., Boch, R., & Kramers, J. (2010). Neotectonic extrusion of the Eastern Alps: Constraints from U/Th dating of tectonically damaged speleothems. *Geology, 38*(6), 483–486.

Pomper, J., Salcher, B. C., Eichkitz, C., Prasicek, G., Lang, A., Lindner, M., et al. (2017). The glacially overdeepened trough of the Salzach Valley, Austria: Bedrock geometry and sedimentary fill of a major Alpine subglacial basin. *Geomorphology, 295,* 147–158.

Poscher, G., & Patzelt, G. (1995). The alluvial fan of the Frauenbachnear Lavant -Late Glacial and Holocene development of an alluvial fan and the valley floor of the Drautal. In E. Schirmer (Ed.), *Quarternary field trips in Central Europe, Eastern Alps Traverse* (pp. 400–401). München: Vlg. F. Pfeil.

Preusser, F., Reitner, J. M., & Schlüchter, C. (2010). Distribution, geometry, age and origin of overdeepened valleys and basins in the Alps and their foreland. *Swiss Journal of Geosciences, 103,* 407–426.

Pugin, A. J. M., Oldenborger, G. A., Cummings, D. I., Russell, H. A., & Sharpe, D. R. (2014). Architecture of buried valleys in glaciated Canadian Prairie regions based on high resolution geophysical data. *Quaternary Science Reviews, 86,* 13–23.

Ratschbacher, L., Frisch, W., Linzer, H. G., & Merle, O. (1991). Lateral extrusion in the Eastern Alps, part 2: Structural analysis. *Tectonics, 10*(2), 257–271.

Reiter, F., Freudenthaler, C., Hausmann, H., Ortner, H., Lenhardt, W., & Brandner, R. (2018). Active seismotectonic deformation in front of the Dolomites indenter, Eastern Alps. *Tectonics, 37,* 4625–4654.

Reitner, J. M. (2003a). Bericht 1998/1999 über geologische Aufnahmen im Quartär auf Blatt 179 Lienz. *Jahrbuch der Geologischen Bundesanstalt, 143,* 516–524.

Reitner, J. M. (2003b). Bericht 2000 über geologische Aufnahmen im Quartär auf Blatt 179 Lienz. *Jahrbuch der Geologischen Bundesanstalt, 143,* 391–397.

Reitner, J. M. (2007). Glacial dynamics at the beginning of Termination I in the Eastern Alps and their stratigraphic implications. *Quaternary International, 164,* 64–84.

Reitner, J. M., Gruber, W., Römer, A., & Morawetz, R. (2010). Alpine overdeepenings and paleo-ice flow changes: An integrated geophysical-sedimentological case study from Tyrol (Austria). *Swiss Journal of Geosciences, 103,* 385–405.

Reitner, J. M., Ivy-Ochs, S., Drescher-Schneider, R., Hajdas, I., & Linner, M. (2016). Reconsidering the current stratigraphy of the Alpine Lateglacial: Implications of the sedimentary and morphological record of the Lienz area (Tyrol/Austria). *Quarternary Science Journal, 65*(2), 113–144.

Röthlisberger, H. (1972). Water pressure in intra-and subglacial channels. *Journal of Glaciology, 11*(62), 177–203.

Röthlisberger, H., & Lang, H. (1987). Glacial hydrology. In A. M. Gurnell & M. J. Clark (Eds.), *Glacio-fluvial Sediment Transfer: An Alpine Perspective*. Chichester: Wiley.

Schmid, S. M., Fügenschuh, B., Kissling, E., & Schuster, R. (2004). Tectonic map and overall architecture of the Alpine orogen. *Eclogae Geologicae Helvetiae, 97*(1), 93–117.

Schmid, S. M., Zingg, A., & Handy, M. (1987). The kinematics of movements along the Insubric Line and the emplacement of the Ivrea Zone. In H. J. Zwart, M. Martens, I. Van der Molen, C. W. Passchier, C. Spiers, & R. L. M. Vissers (Eds.), *Tectonic and Structural Processes on a Macro-, Meso- and Micro-Scale, Tectonophysics*, *135*, Spec. Issue, 47–66. Amsterdam: Elsevier.

Schmidt, T., Blau, J., Grösser, J. R., & Heinisch, H. (1993). Die Lienzer Dolomiten als intergraler Bestandteil der dextralen Periadriatischen Scherzone. *Jahrbuch der Geologischen Bundesanstalt, 136*(1), 223–232.

Seguinot, J., Ivy-Ochs, S., Jouvet, G., Huss, M., Funk, M., & Preusser, F. (2018). Modelling last glacial cycle ice dynamics in the Alps. *The Cryosphere, 12*(10), 3265–3285.

Sprenger, W., & Heinisch, H. (1992). Late Oligocene to Recent brittle transpressive deformation along the Periadriatic Lineament in the Lesach Valley (Eastern Alps): Remote sensing and paleostress analysis. *Annales Tectonicae, 6,* 34–149.

Starnberger, R., Drescher-Schneider, R., Reitner, J. M., Rodnight, H., Reimer, P. J., & Spötl, C. (2013). Late Pleistocene climate change and landscape dynamics in the Eastern Alps: The inneralpine Unterangerberg record (Austria). *Quaternary Science Reviews, 68,* 17–42.

Stork, C. (1992). Reflection tomography in the postmigrated domain. *Geophysics, 57*(5), 680–692.

Strasser, M., Stegmann, S., Bussmann, F., Anselmetti, F. S., Rick, B., & Kopf, A. (2007). Quantifying subaqueous slope stability during seismic shaking: Lake Lucerne as model for ocean margins. *Marine Geology, 240*(1), 77–79. https://doi.org/10.1016/j.margeo.2007.02.016.

Ucik, F. (2005). Die Angaben zu den jungen Talfüllungen im Drau- und Mölltal im Raum Spittal a.d. Drau. In R. Schuster (Ed.), *Arbeitstagung 2005 der Geologischen Bundesanstalt Blatt 182 Spittal an der Drau, Gmünd/Kärnten 12–16 Sept. 2005* (pp. 93–94), Vienna: Geologische Bundesanstalt.

van Husen, D. (1979). Verbreitung, Ursachen und Füllung glazial übertiefter Talabschnitte an Beispielen in den Ostalpen. *Eiszeitalter und Gegenwart, 29,* 9–22.

van Husen, D. (1987). *Die Ostalpen in den Eiszeiten* (pp. 24). Vienna: Veröffentlichung der Geologischen Bundesanstalt, 2.

van Husen, D. (2000). Geological processes during the Quaternary. *Mitteilungen der Österreichischen Geologischen Gesellschaft, 92*(1999), 135–156.

van Husen, D., & Mayer, M. (2007). The hole of Bad Aussee, an unexpected overdeepened area in NW Steiermark, Austria. *Austrian Journal of Earth Sciences, 100,* 128–136.

van Rensbergen, P., de Batist, M., Beck, C., & Manalt, F. (1998). High-resolution seismic stratigraphy of late Quaternary fill of Lake Annecy (northwestern Alps): Evolution from glacial to interglacial sedimentary processes. *Sedimentary Geology, 117,* 71–96.

Vrabec, M., Preseren, P. P., & Stopar, B. (2006). GPS study (1996–2002) of active deformation along the Periadriatic fault system in northeastern Slovenia: Tectonic model. *Geologica Carparthica, 57,* 57–65.

Walach, G. (1993). Beiträge der Gravimetrie zur Erforschung der Tiefenstruktur Alpiner Talfurchen. *Proceedings of the 6th Internationale Alpengravimetrie-Kolloquium, 8,* 83–98.